Manufacturing Letters 35 (2023) 63–67

Contents lists available at ScienceDirect

Manufacturing Letters

journal homepage: www.elsevier.com/locate/mfglet

Passive intensity modulation of a pattern for fabricating near-net shaped features in microscale metal additive manufacturing ☆

Dipankar Behera, Aaron Liao, Michael A. Cullinan *

Walker Department of Mechanical Engineering, The University of Texas at Austin, 204 E Dean Keeton St, Austin 78712, USA

ARTICLE INFO

Article history:
Received 19 September 2022
Received in revised form 21 November 2022
Accepted 12 December 2022
Available online 23 December 2022

Keywords:
Microscale Laser Additive Manufacturing
Spatial intensity modulation
Metal nanoparticle sintering

ABSTRACT

A large variation in part size across the projection area of the microscale selective laser sintering process is caused by non-uniform intensity projected onto the substrate by the digital micromirror device (DMD). A corrective gray scale mask with varying intensities was mapped according to a sintered array of parts. The variance in part size across the area was reduced by as much as 45% by using this technique. This approach can be extended to in real-time process control to create a more uniform distribution of heat and in turn better near net shape parts across the projection area.

1. Introduction

Conventional microfabrication approaches typically rely on expensive physical masks for fabrication of different layers on a substrate. However, digital masks have become more accessible as 'maskless' and inexpensive alternatives to conventional lithography[1]. A digital micromirror device (DMD) is a micro-optoelectromechanical system (MOEMS) which physically allows for spatiotemporal light modulation by generating digital masks. Typically, DMDs have been used in display projection media[2], but over the years it has gained significant traction for use in maskless lithography tools[3–5]. Since the DMD can be used to project various patterns of light, it has found additional applications in laser ablation[6], biomedical imaging[7] and laser microfabrication[8–10].

Microscale selective laser sintering (μ-SLS) is a microscale additive manufacturing (AM) technique that can fabricate true three-dimensional metal structures with a feature-size resolution of 5 μm[11]. This process has primary applications in the microelectronics packaging industry due to its desirable throughput over large areas and ability to create pillar-like structures with high aspect ratios in a layer by layer manner. In the μ-SLS process, a coating mechanism deposits a layer of metal nanoparticle onto the substrate[12]. A DMD with focusing optics projects a laser in a desired pattern onto the coated substrate. The region exposed by the laser is heated up and the part is formed through the process of solid state diffusion. The coating and sintering processes are repeated to fabricate a structure with desired features. Further details about the μ-SLS tool can be found in previous works by the authors[11].

This work presents an intensity modulation approach where the pattern that is projected through the DMD can be corrected to account for the non-uniformities of the sintered layer. The novelty of the process is in implemented the pattern correction and intensity modulation using the feedback from the sintered layer, which allows for a better control of the near-net shape of microscale parts.

2. Motivation behind this work

A digital micro-mirror device uses several MOEMS mirrors which express 0 and 1 states that turn individual mirrors 'off' and 'on' respectively. When it is 'on' the light is directed towards the corresponding pixel for projection and when it is 'off' the light is directed towards a collector connected to a heat sink. The DMD enables the μ-SLS process to achieve high throughput patterning by simultaneously exposing multiple features as opposed to raster scanning across an area. In addition to providing binary intensity, the DMD can also achieve gray-scale intensities (values between 0 and 1) through pulse width modulation[13]. In the μ-SLS process this capability can be utilized to actively or passively control the thermal profile to better produce near net shape parts across the sintering area.

However, inherent non-uniformities of the DMD intensity over the entire projection area can lead to insufficient sintering of

☆ This document is the results of the research project funded by the National Science Foundation.

* Corresponding author.
E-mail address: michael.cullinan@austin.utexas.edu (M.A. Cullinan).

https://doi.org/10.1016/j.mfglet.2022.12.002

certain regions of the substrate. These non-uniformities are a result of fabrication inaccuracies, micromirror damage, thermal aberrations, and optomechanical misalignments, and vignetting. DMD intensity non-uniformities lead to the following issues in the μ-SLS process - (1) Inability to fabricate 2.5/3D features with uniform cross section, (2) Insufficient sintering leading to poor adhesion to the substrate, and (3) Difficulty in fabricating high aspect ratio microscale features due to inaccurate layer stacking. These issues collectively degrade the near-net shape of the microscale structure that can be fabricated with the μ-SLS process which is undesirable. Some improvement can be expected by using an optical homogenizer in beam path as shown by Sun et al. [9] for vat photopolymerization processes, but that leads to additional optical power losses as discussed in optical design of the μ-SLS process[14].

The challenges due to non-uniform intensity profile of the DMD have been reported in previous maskless lithography approaches [3,15]. Rajan et al.[16] and Yoon et al.[17] addressed similar challenges in the maskless fabrication approaches by capturing the intensity output of the projection feature and correcting for the illumination profile in the fabrication step. However, these approaches are system specific and require ex-situ calibration. Furthermore, the variation in the near-net shape of an AM feature can also be caused by thermal aberrations within the DMD, light-matter interaction and imprecise optics. Therefore, in this study, we present a closed-loop method to fabricate near-net shape parts across the exposure area of a DMD used for the μ-SLS process by implementing intensity correction based on the actual sintered features.

3. Materials and methods

The digital micromirror device used in the μ-SLS process is a DLP-6500 chipset (Texas Instruments) with beam-shaping and illumination optics [11]. Binary and grayscale images can be uploaded to the system via the GUI, and projected on the substrate with up to a maximum bit depth of 8. Based on the bit-depth, grayscale images are effectively converted into multiple binary images with varying switching frequencies of individual pixels. For this study, Ag nanoparticle ink (Novacentrix) was coated on a glass substrate and was positioned under the DMD. A dot array (Fig. 1a) was projected using the DMD on the Ag NP ink bed under the following lasing conditions - Voltage (V) = 17–20 V (floating), Current (I) = 20–35 A, Bursts (B) = 150, Duty cycle (D.C.)= 10%, pulse repetition rate (PRR) = 100 Hz. This corresponds to average irradiances ranging from of 60–100 W/cm^2. After the desired spots were sintered (Fig. 1b), the NP ink was allowed to dry at 100 °C on a hot plate. Next, the samples were positioned on a fixture and imaged under a Motic PSM-1000 optical microscope with a 20x objective lens. As seen in Fig. 1b, there is a large non-uniformity between the diameters of the dots in the center and the dots towards the edges. Furthermore, the dots at the last edge rows and columns are virtually non-existent. This can be attributed to the issues identified in the previous section. The dots at the edge were not fully sintered which led to poor adhesion to the substrate and eventual lift-off while removing the excess ink with a solvent. This also presents significant challenges while stacking multiple layers in this layer-by-layer manufacturing process.

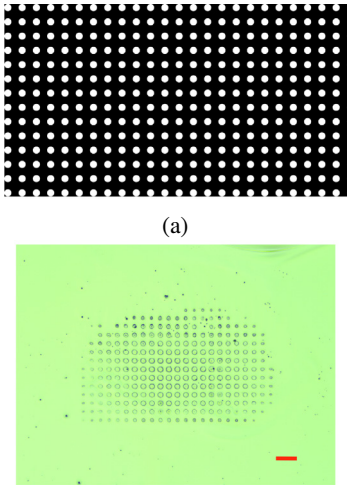

(a)

(b)

Fig. 1. (a) Original binary mask with 40 μm circles and 80 μm pitch (b) [Scale bar = 160 μm] Optical microscope image of the features as obtained by projecting the dot array mask on a nanoparticle ink bed without any intensity modulation for laser parameters V = 17 V, I = 20 A, PRR = 100 Hz, Duty Cycle = 10%.

To compensate for this difference in diameters, the non-uniformities in the intensity profile of the incident light must be adjusted. As discussed previously, the DMD generates the desired pattern by independent switching the micromirrors into 'on/off' stages. With the very basic configuration, the intensities from the micromirrors are produced by pulse width modulating them over a specified refresh time. The features obtained in Fig. 1b correspond to a 1-bit depth image since it is a binary image. The relative brightness of the pixel can be written in up to 8 bits (allows for 256 unique combinations of ones and zeros), which correspond to varying on/off durations. This effectively encodes the different intensities of gray scale.

A straightforward way of mapping the intensity profile of the DMD output is using a beam profiler. However, the short burst durations and the minimum laser threshold fluence led to less reproducible data using this approach.Therefore, an alternative approach was implemented where the unmodulated image shown in Fig. 2a was used as the 'ground truth'. Then, the original dot array was used as a mask to obtain a fused image and nominally evaluate the alignment of the two images (as shown in Fig. 2b). Next, the sintered image was converted into a binary image and broken down into a 4 x 8 array as shown in Fig. 2c. The resulting images are then processed to find the mean of the areas covered by the circles obtained by applying a binary mask. The regions with smaller circles had less number of 'dark' pixels and higher number of 'bright' pixels.

The processing step assigned a mean pixel intensity to each sub-images. The resulting pixel matrix was normalized across a range of grayscale values from 0 to 1. The original binary mask was multiplied with the inverted pixel matrix to obtain a grayscale mask which has pixels with varying intensity. Fig. 2d shows the original image which was used to back calculate the expected intensity variation, and Fig. 2e shows the dot array with the intensity mask applied. The mask is the inverse of the resultant intensity map to account for darker regions at locations where the circle diameter is larger and brighter regions where the circle diameter is smaller. A limitation of this approach is that the overall resolution of the intensity map would depend on the number of the original sub-images, and hence, a potentially higher accuracy intensity mask can be obtained by sub dividing the original image into smaller sections.

4. Results and discussions

The new mask as shown in Fig. 2e was projected on to the coated substrate. Two test artifacts fabricated with the modulated intensity profiles are shown in Fig. 3b and c. A qualitative comparison between the sintered parts fabricated without any intensity

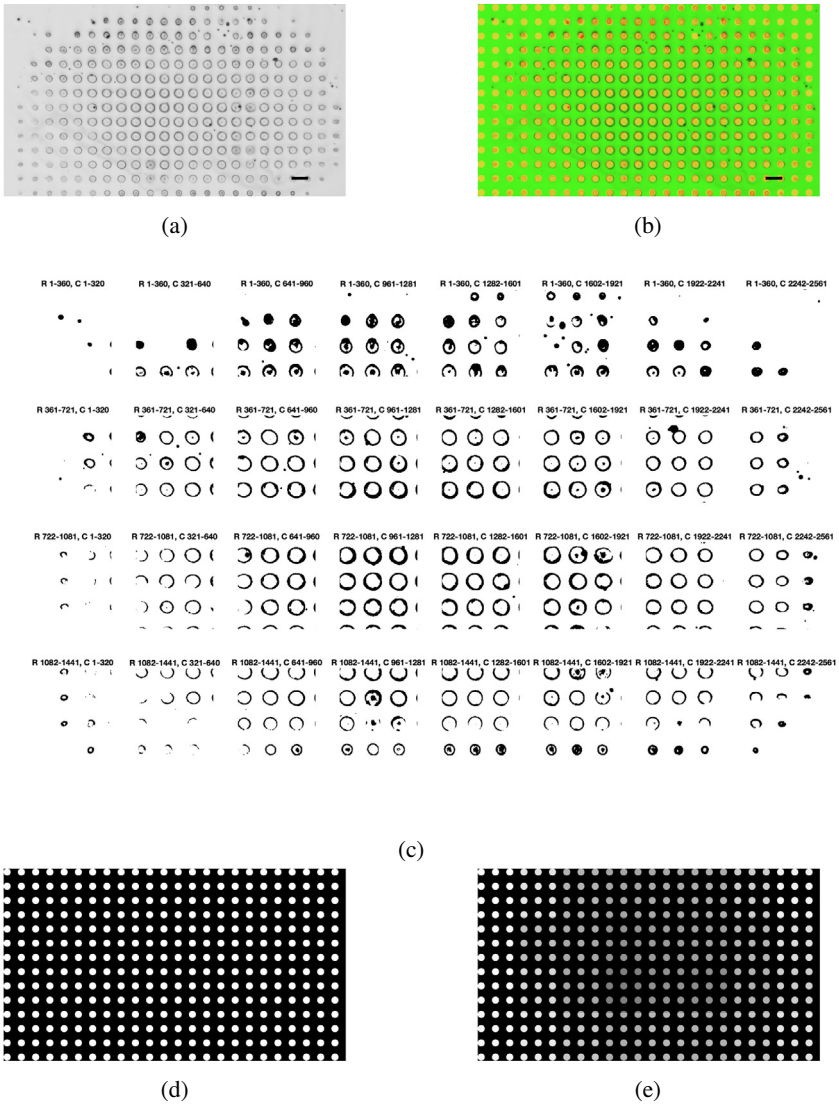

Fig. 2. [Scale bar = 80 μm] (a) Resized Optical microscope image of the dot array shown in Fig. 1b (b) Fused image of the unmodulated dot array with the original binary mask. (c) Figure showing the 8 × 4 sub-images sintered image was processed and disaggregated. (d) Original binary mask (e) Modulated grayscale mask for projection obtained by processing the unmodulated images.

modulation (Fig. 3a), and with intensity modulation (Fig. 3b and c) shows the difference in the near net shape of the patterned layer. All the samples were processed using the same approach discussed previously to obtain the intensity map and the modulated grayscale image. A qualitative comparison of the images shown in Fig. 3-a-c shows that the dot array obtained using the modulated mask has a more uniform distribution. Post processing these samples also showed that the likelihood of the circles around the edges being washed off during the excess ink removal step was lower which can be attributed to better sintering of the features at those locations. This also ensures that the features sintered in the subsequent layers will have a higher chance of adhering to the previous layers due to a uniform localized heat spread on the nanoparticle bed.

The images shown in Fig. 3a-b were divided into sub-figures using the same approach shown in Fig. 2c and a distribution of the intensity map was plotted as shown in Fig. 4. In this plot, the unmodulated sample (Fig. 3a) has a heavier bottom tail compared to the two modulated samples (Fig. 3b and c). The variance in the dot array distribution are 7.2×10^{-4} and 5.4×10^{-4} for modulated test 1 and test 2 respectively, compared to the 9.8×10^{-4} value for the unmodulated images. The heavier tail for unmodulated sample shows that the non-uniformities in the laser material interactions produce circles with different diameters across the array. The reduction in variance by 45% shows that the grayscale modulation of light improves the uniformity in the diameters of the circles. Therefore, this approach assists in obtaining a better near-net shaped part by distributing the heat across the nanoparticle ink bed more uniformly.

A significant advantage of this approach is that it captures the non-uniformities in the processing step as well, which can come from variations in the coating thickness, optomechanical misalignments and thermal aberrations due to continued operation. However, using the sintered image as a model input parameter and applying the processing steps discussed above captures these non-uniformities as well as the laser material interaction. The proposed passive intensity modulation approach allows the in situ calibration of the layer information during of the fabrication of microscale 3D printed parts. Compared to the use of additional metrology system which measures part quality and layer fidelity, the proposed methodology is faster and incorporates the imperfections of the laser-material interaction. This approach can be imple-

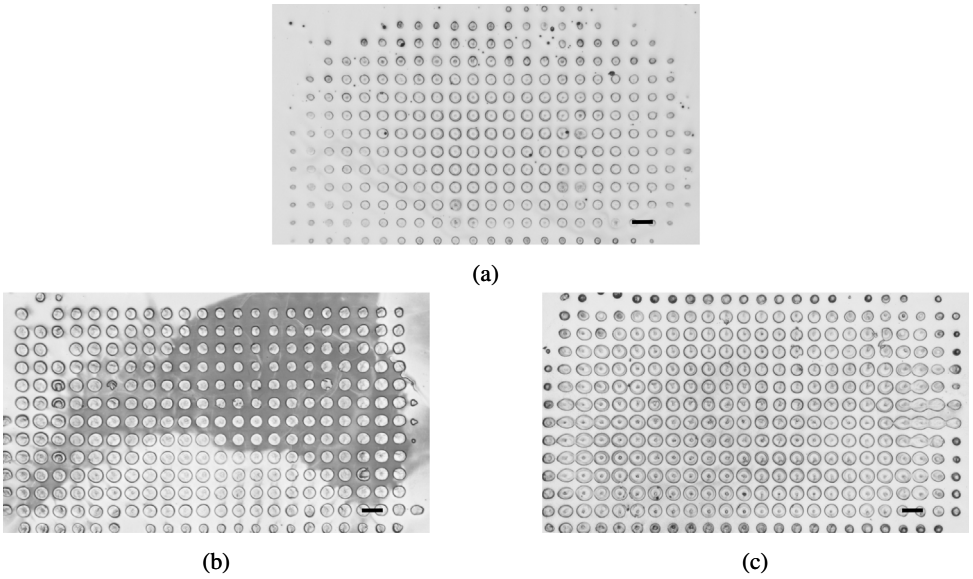

Fig. 3. [Scale bar = 80 μm] (a) Original dot array without any modulation (b) Dot array with modulation - Test artiFact 1 (c) Dot array with modulation - Test artiFact 2. The two test artifacts are repeated tests using the same modulation approach.

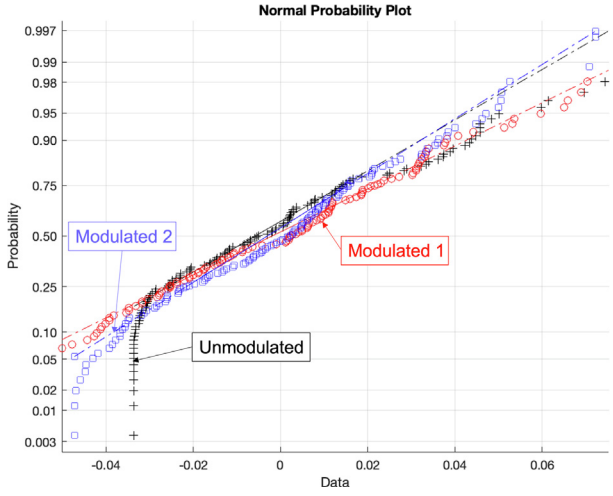

Fig. 4. Normal probability plot of the unmodulated and modulated dot arrays. Modulated Test 1 and Test 2 are two repeated tests with the same modulation parameters.

mented in a passive manner by developing a process control model for modulating the n^{th} layer based on the information from the $(n-1)^{th}$ or in an active manner by implementing the approach in real-time.

5. Conclusions

This study established a technique to address the variance in feature sizes across the projection area onto a substrate for the microscale selective laser sintering process. The key contributions of this work are as follow -

· An intensity modulation technique was developed which used a compensating gray-scale mask from the distribution of feature sizes obtained using a binary mask. Images of an array of sintered parts were processed to determine mean pixel intensities in disaggregated regions across the projection area, and a corresponding gray-scale intensity value was assigned to each region.

· This technique treats the sintering process as a black box with intensity distribution as the input and part size uniformity as the output. As a result, the negative contribution to near net shape parts from variation in deposited ink thickness, thermal profile, defects in the micro mirror array in DMD, and optomechanical misalignment are targeted using this black box.

· The approach used in this study focuses on a correcting a single layer of parts created by a binary mask, but it can be extended to multiple layers by generating gray-scale masks in a feedback loop according to the observed part size distribution in the previous sintered layer.

Declaration of Competing Interest

The authors declare that they have no known competing financial interests or personal relationships that could have appeared to influence the work reported in this paper.

References

[1] Diez S. The next generation of maskless lithography. In: Douglass MR, King PS, Lee BL, editors. Emerging digital micromirror device based systems and applications. (San Francisco, California, United States); Mar. 2016. p. 976102.
[2] Sampsell JB. Digital micromirror device and its application to projection displays. J Vacuum Sci Technol B: Microelectron Nanometer Struct 1994;12:3242. Nov..
[3] Love JC, Wolfe DB, Jacobs HO, Whitesides GM. Microscope projection photolithography for rapid prototyping of masters with micron-scale features for use in soft lithography. Langmuir 2001;17:6005–12. Sept..
[4] Musgraves JD, Close BT, Tanenbaum DM. A maskless photolithographic prototyping system using a low-cost consumer projector and a microscope. Am J Phys 2005;73:980–4. Oct..
[5] Martinsson Hans, Sandstrom Tor, Bleeker Arno J, Hintersteiner Jason D. Current status of optical maskless lithography. J Micro/Nanolithogr, MEMS, and MOEMS 2005;4:1–15. Jan..
[6] Heath DJ, Grant-Jacob JA, Feinaeugle M, Mills B, Eason RW. Sub-diffraction limit laser ablation via multiple exposures using a digital micromirror device. Appl Opt 2017;vol. 56. p. 6398–6404. Publisher: OSA.
[7] Zheng C, Zhou R, Kuang C, Zhao G, Yaqoob Z, So PTC. Digital micromirror device-based common-path quantitative phase imaging. Opt Lett 2017;42:1448. Apr..
[8] Singh-Gasson S, Green RD, Yue Y, Nelson C, Blattner F, Sussman MR, Cerrina F. Maskless fabrication of light-directed oligonucleotide microarrays using a digital micromirror array. Nat Biotechnol 1999;17:974–8. Oct..
[9] Sun C, Fang N, Wu D, Zhang X. Projection micro-stereolithography using digital micro-mirror dynamic mask. Sens Actuat A: Phys 2005;121:113–20. May.

[10] Rahlves M, Kelb C, Rezem M, Schlangen S, Boroz K, Gödeke D, Ihme M, Roth B. Digital mirror devices and liquid crystal displays in maskless lithography for fabrication of polymer-based holographic structures. J Micro/Nanolithogr, MEMS, and MOEMS 2015;14:041302. July.
[11] Roy NK, Behera D, Dibua OG, Foong CS, Cullinan MA. A novel microscale selective laser sintering (μ-SLS) process for the fabrication of microelectronic parts. Microsyst Nanoeng 2019;5:64. Dec..
[12] Behera D, Liao D, Cullinan MA. Slot-die coating operability window for nanoparticle bed deposition in a microscale selective laser sintering tool. J Micro Nano-Manuf 2020;8:041012. Dec..
[13] Dudley D, Duncan WM, Slaughter J. Emerging digital micromirror device (DMD) applications. In: Urey H, editor. MOEMS Display and imaging systems. (San Jose, CA); , Jan. 2003. p. 14.
[14] Roy NK, Behera D, Dibua OG, Foong CS, Cullinan MA. Single shot, large area metal sintering with micrometer level resolution. Opt Exp 2018;26:25534. Oct..
[15] Miyamoto N, Shimakage M, Morimoto T, Kadota K, Sugawa S, Ohmi T. A rapid prototyping of real-time pattern generator for step-and-scan lithography using digital micromirror device. In: 2007 International conference on field-programmable technology; Dec. 2007. p. 305–8. Journal Abbreviation: 2007 International Conference on Field-Programmable Technology.
[16] Kattipparambil Rajan D, Raunio JP, Karjalainen MT, Ryynänen T, Lekkala J. Novel method for intensity correction using a simple maskless lithography device. Sens Actuat A: Phys 2013;vol. 194. p. 40–46.
[17] Yoon J, Kim K, Park W. Modulated grayscale UV pattern for uniform photopolymerization based on a digital micromirror device system. Appl Phys Lett 2017;111:033505. July.